Polarization relaxation kinetics and 180° domain wall dynamics in ferroelectric thin films

C. S. Ganpule,* A. L. Roytburd,† V. Nagarajan, B. K. Hill, S. B. Ogale, E. D. Williams, and R. Ramesh‡
Materials Research Science and Engineering Center, University of Maryland, College Park, Maryland 20742

J. F. Scott
Symetrix Center for Ferroics, Earth Sciences Department, Cambridge University, Downing Street, Cambridge, CB2 3EQ, United Kingdom
(Received 16 April 2001; published 29 November 2001)

The time-dependent relaxation of remanant polarization in epitaxial lead zirconate titanate [$Pb(Zr_{0.2}Ti_{0.8})O_3$,PZT] ferroelectric thin films, containing a uniform two-dimensional grid of 90° domains (*c* axis in the plane of the film), is examined using voltage-modulated scanning force microscopy. 90° domain walls preferentially nucleate 180° reverse domains during relaxation, which grow and coalesce as a function of relaxation time. Relaxation is seen to saturate at different levels depending on the write voltage. Late (saturation) stages of relaxation are accompanied by pinning and faceting of the domain walls (drastically reducing the wall mobility), which is direct evidence of the role of defect sites and crystallographic features on polarization relaxation. The kinetics of relaxation is modeled through the nucleation and growth Johnson-Mehl-Avrami-Kolmogorov theory with a decreasing driving force.

DOI: 10.1103/PhysRevB.65.014101 PACS number(s): 77.22.Ej, 77.80.Dj, 77.84.−s

I. INTRODUCTION

At present there is considerable interest in ferroelectric thin films as a medium for nonvolatile data storage.[1] In particular much attention has been paid to investigating high-density gigabit data storage using scanning probe techniques.[2] The ferroelectric element in these storage media is subject to progressive loss of polarization, commonly referred to as ''polarization relaxation.'' Measurement of the remanant polarization of a macroscopic capacitor is one of the ways to study the polarization loss as a function of wait time. However, this may not necessarily lead to a complete understanding of the underlying domain evolution in the ferroelectric film. It is important to supplement the information obtained from such a macroscopic experiment with high-resolution domain images during the relaxation process in order to understand the mechanisms governing backwitching. Early studies on the microscopic origins of polarization reversal using scanning probe microscope techniques[3] show that they have the potential for quantifying the physical origin of the relaxation kinetics. In many of these studies the top electrode is eliminated to obtain the highest resolution possible and more importantly to artificially speed up the relaxation process. Absence of a top electrode implies that the film polarization is forced predominantly into a uniform orientation thereby leading to a net driving field for the unstable reverse poled parts of the film. In a recent publication[4] we showed the evolution of reversed domains in epitaxial lead zirconate titanate thin films grown on $SrTiO_3$ with oxide La-Sr-Co-O electrodes. It was seen that reversal proceeds by nucleation and growth of reverse 180° domains. These reverse domains were found to nucleate at the interface of *c* domains and *a* domains in the tetragonal $Pb(Zr_{0.2}Ti_{0.8})O_3$ (PZT) thin film.[5] A stretched exponential fit was found to be a well-suited functional fitting form for the time dependence of the reversed fraction. In this report we have attempted to further probe the nanoscale features of 180° domain wall dynamics and relate its topology and dynamics to the crystallography and defect structures in the film and therefore to the overall relaxation kinetics. Johnson-Mehl-Avrami-Kolmorogov (JMAK) theory is a useful approach for systems exhibiting nucleation and growth routes of phase change kinetics.[6] In this article we attempt to apply this theory to the polarization reversal in the ferroelectric thin films.

II. EXPERIMENT

The ferroelectric films consisted of epitaxial 4000-Å-thick PZT (0:20:80) films grown on a single-crystal $SrTiO_3$ (STO) substrate with a 500-Å-thick La-Sr-Co-O (LSCO) oxide layer as the bottom electrode. $PbZr_{0.2}Ti_{0.8}O_3$ thin films were deposited at 650 °C and 100-mTorr oxygen partial pressure on (001) epitaxial grade STO substrates (Crystec. GmbH, Germany) by pulsed laser deposition (PLD). The details of the deposition process are given elsewhere.[5] The samples were cooled at a rate of 1 °C/min from the growth temperature. The thickness of individual layers were confirmed by Rutherford backscattering (RBS) and transmission electron microscopy (TEM).

X-ray diffraction (XRD) experiments for all samples were done on a four-circle Siemens D5000 diffractometer with monochromatic Cu $K\alpha$ radiation. Crystallographic characterization was accomplished with standard θ–2θ scans, θ rocking curves, and ϕ scans, with angular resolutions of ~0.1°, ~0.1°, and ~4°, respectively. Epitaxial growth in the samples was established from ϕ scans and the presence of only 00*l* type reflections in the θ–2θ diffraction pattern. The PZT film contained a uniform two-dimensional (2D) grid of 90° domains (i.e., *c* axis in the plane of the film). Such 90° domains have been shown to have a strong impact on the hysteretic polarization behavior of ferroelectric films.[7] Due

 ©2001 The American Physical Society

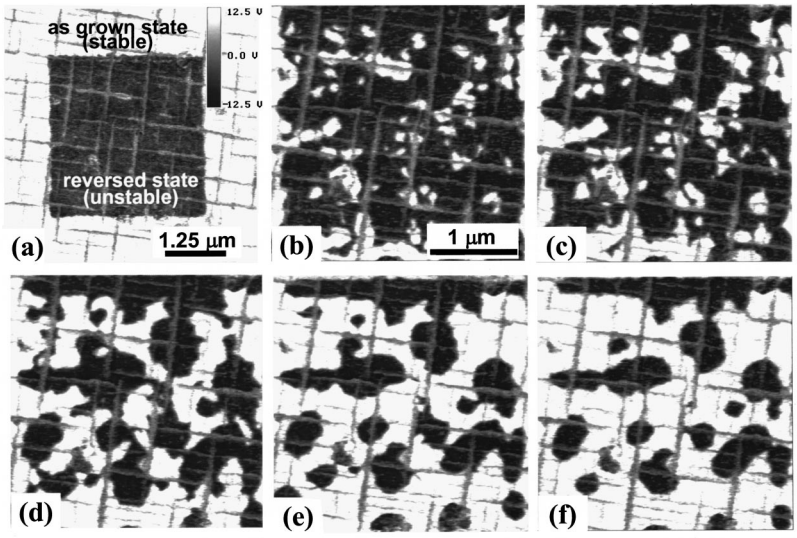

FIG. 1. (a) Piezoresponse image from a 5 μm$\times$5 μm area of the $Pb_{1.0}Zr_{0.2}Ti_{0.8}O_3$ sample showing the as-grown regions (light contrast) and the reverse poled region of 3 μm$\times$3 μm in the center (dark contrast). (b)–(f) Piezoresponse images from the 3 μm$\times$3 μm region from (a), which was switched into the opposite polarization (with respect to the as-grown state) state by scanning the surface with the tip biased at -10 V. Images taken after wait times of (b) 6.1×10^3, (c) 9.2×10^3, (d) 2.4×10^4, (e) 1.1×10^5, and (f) 2.8×10^5 s.

to the absence of a top electrode the polarization and piezoresponse hysteresis loops show a marked asymmetry, thereby indicating a built-in internal field. The value of this field was calculated to be around 3.5×10^6 V/m.[4]

Voltage-modulated scanning force microscopy[8] has been employed recently to study the piezoelectric effect and to image and modify the domain structure in thin-film samples. For our experiments we used a commercial Digital Instruments Nanoscope IIIA Multimode atomic force microscope (AFM) equipped with standard silicon tips (radius 5–15 nm) coated with nickel silicide for electrical conduction. All images were acquired at room temperature in ambient atmosphere.

III. RESULTS

Piezoresponse images of the surface of the as-grown PZT film (Fig. 1) show the presence of long needlelike orthogonal structures that have been identified to be 90° twin domains (denoted by ''T'' in the image), which form to relax the strains associated with lattice mismatch and phase transformation from the cubic to the tetragonal (ferroelectric) phase.[9,10] The image contrast in between the needlelike regions is uniformly bright, suggesting that the entire region is prepoled in a specific direction. The as-grown polarization vector in the sample was switched into the opposite state by scanning the surface of the film (3 μm$\times$3 μm) with the AFM tip biased at -8 V (scan speed 1 Hz) leading to a strong change in the image contrast from bright to dark as observed in the inner part of Fig. 1(a). We observed this switched state (in the *c*-axis regions of the film) begin to relax back to the original bright state, the kinetics of which is the focus of this paper. Piezoresponse images were recorded from the same region as a function of time from a few minutes to several days. The polarization spontaneously reversed its direction as illustrated in the sequence of piezoresponse images in Figs. 1(b)–1(f). The internal field present due to the asymmetry of the electrode structure drives the reversal. Nucleation of the reverse domains was found to occur preferentially at the twin boundaries, as was also noticed in an earlier work.[5] The process of nucleation of reverse domains was followed by the growth of these regions to cover an increasing area of the film. It is to be noted that the reversal did not proceed completely to the fully poled as-grown state, but rather to a saturation value for the fraction of ''unstable'' remanant black domains within a matrix of stable, reversed, as-grown ''white'' domains depending on the writing field. However, this state was only stable at room temperature. Heating the film to 400 °C caused the domain structure to revert to the fully poled white state. These observations were found to be repeatable in several experiments conducted over various parts of the sample.

To study the effect of the dc writing voltage, the above experiment was repeated for the write voltages of -10, -12, and -14 V. As shown in Fig. 2, the effect of dc ''write'' voltages is to dramatically alter the net reversed fraction within the experimentally observable time. It was seen from the domain images acquired for each of these write voltages that the nucleation density is reduced with higher write voltages. In order to study the local phenomena in greater detail we repeated the relaxation experiment on *c*-axis regions bounded on all four sides by *a*-axis domains. This helped ensure that the nanoscale domain dynamics that was being

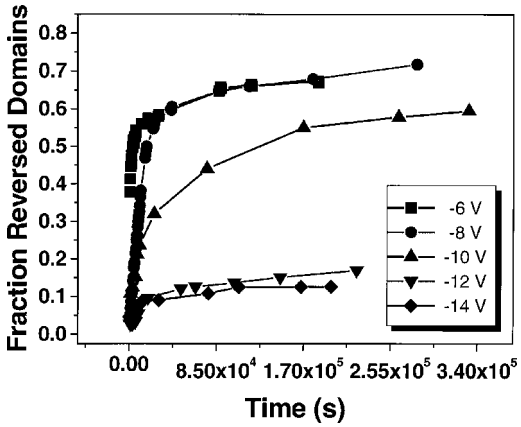

FIG. 2. Fraction reversed domains as a function of the dc ''write'' voltage.

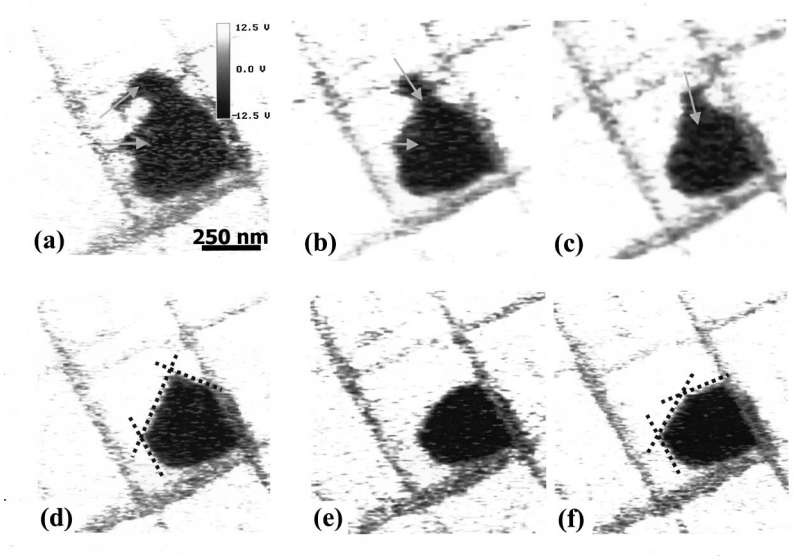

FIG. 3. (a)–(c) Relaxation in a ''single cell.'' Data illustrate the role of curvature in governing the local velocity of the 180° domain wall. Arrows indicate the direction of the velocity of the moving wall. This normal velocity slows down as the curvature of the wall decreases and faceting takes place as seen in (d) and (f). Images taken after wait times of (a) 4.6×10^3, (b) 8.7×10^3, (c) 1.2×10^4, (d) 2.6×10^4, (e) 7.5×10^4, and (f) 1.6×10^5 s.

investigated was not affected by growth of reverse domains from neighboring regions. Curvature of the phase boundary has been known to play a key role in modifying the normal velocity of the wall.[11] The existence of a surface tension implies a force per unit area, proportional to the mean curvature, acting at each point on the wall. This force will cause the walls to move, with a velocity proportional to the local curvature. The effect of local curvature on the 180° domain wall velocity can be seen in Figs. 3(a)–3(f). When the curvature of the areas marked by the arrows is large, the normal velocity of that part of the wall is very high, but when the curvature decreases to very small values as the wall becomes progressively flatter, the wall velocity decreases and finally goes to zero when the wall becomes faceted. Clearly there are two possible ways in which the transformed region can grow into the original unstable areas. At early times as seen schematically in Fig. 4(a), the growing cylindrical regions imply a decreasing volume free energy accompanied by an increasing surface energy as the surface area of the individual white nuclei increases. At later times after coalescence produces varying topologies of the 180° domain wall, it can be observed [Fig. 4(b)] that the transformed volume can increase while being accompanied by a reduction in the surface area of the 180° domain wall as regions of unstable ''black''

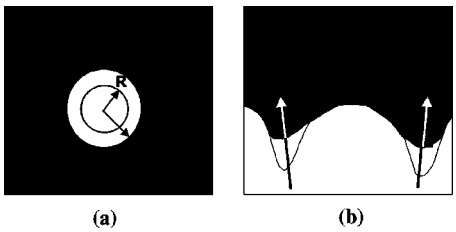

FIG. 4. (a) Change of curvature as the ''white'' reversed domain grows in size at early times. (b) Change of curvature of the 180° domain wall at areas marked by the arrows as transformation proceeds by the white stable region growing into black unstable regions at areas of high curvature of the unstable state (at late times of relaxation).

state get transformed. In this case the overall free energy decreases much more rapidly as both the surface energy and the volume energies decrease. Thus the local domain wall velocity in this case is very high. Local curvature therefore affects the rate of transformation.

In the final stages of the growth, the curvature of the domain wall tends to zero and a faceted structure is observed. This faceted structure represents a metastable state for the domain wall as it lies along the low-index planes of the tetragonal crystal. As an illustration consider the series of domain images for relaxation of a single 300-nm ''cell'' in Figs. 5(a)–5(e). As can be observed in Figs. 5(d) and 5(e), the domain wall is seen to lie along the (110)-type and (100)-type planes of the crystal, which seems to suggest that these planes represent the low-energy configurations for the domain wall. These facets are, however, metastable states, and their stability is limited by thermal fluctuations of the wall. The domain wall velocity and hence the transformation rate for this ''single-cell'' region shows a marked slow down at around $t=2\times10^5$ s [Fig. 5(f)]. The domain image corresponding to this time scale is clearly faceted as seen in Fig. 5(d). It can be also seen that the transformation rate then increases before tapering off once again as the domain structure settles into another faceted metastable state [Fig. 5(e)].

Recently, Yang *et al.* have calculated the surface energy of a 180° domain wall by observing the bowing of a pinned wall using optical observations.[12] Figures 6(a)–6(i) shows the transformation in a single ''cell'' 500 nm wide. The domain wall is seen to meander across from the nucleation site inside one of the sides towards the opposite *a*-domain wall until it gets pinned by defect sites as observed in Fig. 6(i). In the early stages there is enough driving force for the domain wall to overcome the pinning sites as can be seen in the series of images Figs. 6(b)–6(h). However, as the relaxation proceeds to later stages, the driving force is exhausted and the wall, unable to break free from the pinning sites, bows out. The difficulty of estimating this small driving field at the end of the relaxation prevents an accurate estimation of the wall energy. However, if we assume that Fig. 6(i) represents

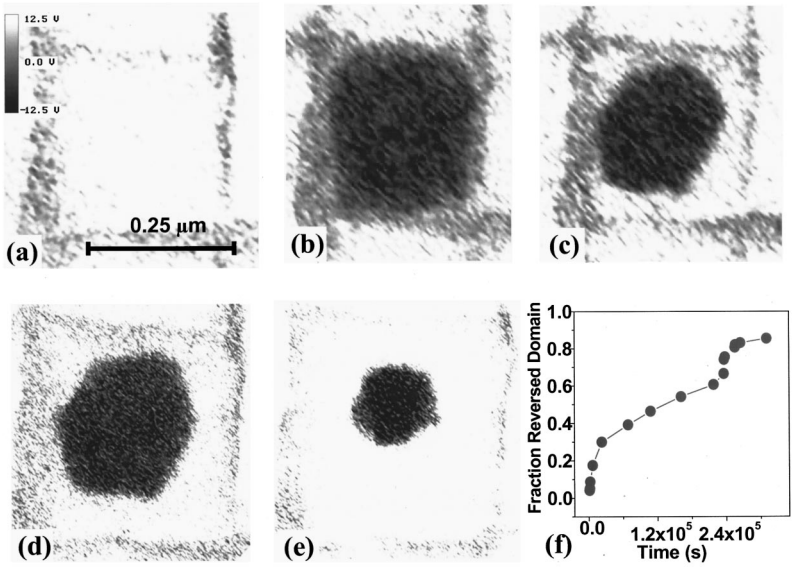

FIG. 5. (a) Piezoresponse scans of a single cell in $Pb_{1.0}Zr_{0.2}Ti_{0.8}O_3$. (b)–(d) illustrate the spontaneous reversal of polarization within this region after wait times of (b) 1.01×10^3, (c) 1.08×10^5, (c) 1.61×10^5, and (d) 2.55×10^5 s. The faceting can be clearly seen in (c), (d), and (e). (f) Transformation-time curve for the data in (b)–(e).

a state of saturation for relaxation in the film, then we can estimate the wall energy Γ as $\Gamma = RP_sE(1-\alpha) \approx 0.12\ \mathrm{J/m^2}$, where α represents the fraction of unstable (''black'') region of the film.

IV. DISCUSSION

While a study of the nanoscale origins of polarization reversal in ferroelectric thin films is a relatively new field, there have been reports in the past on a logarithmic linear time-dependent decay of polarization, suggesting a broad distribution of relaxation times.[13] Other studies in the past, including ours, have indicated a stretched exponential decay of the remnant polarization, suggesting a random-walk-type mechanism of retention loss.[3,4] However, a fundamental explanation of such a stretched exponential behavior appears to be complicated, since in much of the earlier work,[14] stretched exponential type relaxation has been correlated to the movement or relaxation of point objects (spin in magnetic spin glasses, hydrogen in amorphous silicon, etc.). Experimental evidence as presented in this paper shows clear evidence of a nucleation and growth mechanism. Hence, while much of the early work provides an empirically accurate description of the functional fit of the observed kinetics, we have made an attempt, in this report, to understand and model the physical origin of relaxation and the kinetics of coalescence in the later stages. The difficulty in interpreting the present picture of domain nucleation and growth during relaxation is caused by the fact that both the thermodynamic stimuli for relaxation and the kinetics of domain evolution change during relaxation.

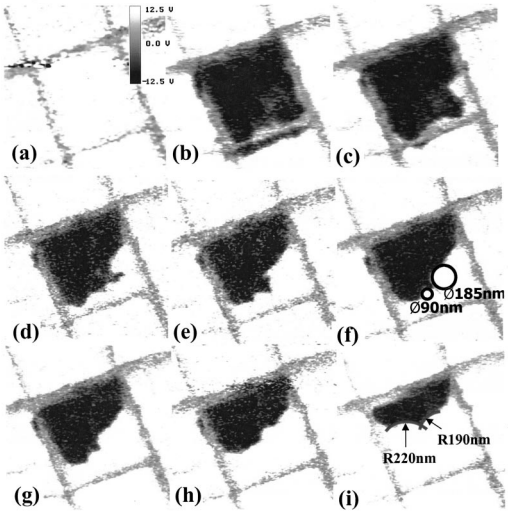

FIG. 6. Polarization relaxation images in (a) a ''cell'' of width 500 nm for times (b) 2.0×10^3, (c) 6.6×10^3, (d) 1.4×10^4, (e) 1.8×10^4, (f) 2.2×10^4, (g) 2.3×10^4, (h) 3.0×10^4, (i) 2.1×10^5 s. Pinning and bowing of the 180° wall can be observed in (d)–(i).

The thermodynamic driving force for relaxation is a result of the built-in field due to charge redistribution within the electrode. In the as-grown state this built-in field is compensated by the film polarization, so that the net electrostatic field in the film is close to zero. The polarization charge is considerably less than P_s due to the effect of internal screening near the interface. Since this poled state can exist for a long time and can be repeatedly obtained after reheating the sample, it is to be naturally assumed that this is close to the ''stable'' state of the film and that the electrostatic field in the film is absent (or close to zero) for this state. After ''writing'' or switching the polarization vector under an external dc field, an unstable state of polarization is created which then relaxes toward the as-grown stable state. However, the applied voltage should affect the distribution of charges in the electrode. Therefore the field in the film after writing but just before relaxation can be expressed as $E_i(1-\alpha)$, where E_i is the built-in field which would exist if the external field had not changed the charges within the electrode. The factor α depending on the voltage of writing (and possibly the duration) characterizes the decrease in the field due to a change in the electrode charge distribution. (Gruverman and Tanake similarly observed suppression of relaxation in a recent publication.[15])

During relaxation, the net charge at the interface decreases due to reversal of polarization. Since the charge can quickly redistribute within the electrode, its localization may be ignored. Thus the reversed polarization results in a decrease of the mean field within the film proportional to the fraction of reversed domains, i.e., $E=E_i(1-\alpha-f)$, where f is the fraction of reversed domains. This progressive decrease in the field with relaxation is an important factor, which determines the thermodynamic driving force for the relaxation. Experimental proof of this trend is the decreasing curvature of domain walls bowing between pinning points. The estimation of this field in the film during a stage that approaches saturation in Fig. 6(i) gives $E(f)=0.28E_i$. This is a small fraction of the built-in field estimated from the shift of the hysteresis loop.

The decrease in the mobility of the domain wall is the second reason for the incomplete relaxation of the written state. The direct observation of pinned walls at small fields and their noncrystallographic orientation allows us to suggest that the main controlling mechanism of domain wall mobility is the overcoming of pinning points in the field. However, when the effective field approaches zero, the domain wall is closer to equilibrium and crystallographically oriented facets are formed. The domain wall movement should then require 2D nucleation and this diminishes the mobility dramatically.

The analysis of the experimental results which is presented above allows us to formulate the following description of the relaxation process. We assume that the relaxation proceeds via growth of cylindrical domains simultaneously nucleated on the twins. Then the time evolution of reversed domain fraction is described as

$$f=1-e^{-NV(t)}, \tag{1}$$

where N is the surface density of nucleation centers, $V(t)$ is the volume of a single domain at time t. Equation (1) follows from the general theory of nucleation and growth (JMAK) under the condition that the nucleation rate is a δ function of time at small t. Equation (1) shows that the overall kinetics follow the kinetics of growth of individual domains, but at the same time it also takes domain impingement into account.

Since the velocity of growth of cylindrical domains through the thickness is much larger than along its radius, the problem can be reduced to a two-dimensional one. We therefore consider the growth of a system of disks in the interface plane as shown in Fig. 7(a). Then in Eq. (1), $V(t)=\pi[R(t)]^2$ and N is a surface density of nucleation centers. The growth of a single reversed domain is shown schematically in Fig. 7(b).

If domain growth is controlled by thermoactivated overcoming of pinning points [as illustrated in Fig. 7(c)] and does not need 2D nucleation due to the roughness of the wall (as seen experimentally), it is described by a linear relation between the growth velocity dR/dt and the thermodynamic driving force f_T,

$$\frac{dR}{dt}=-Kf_T=-K\frac{1}{2\pi Rh_f}\frac{\partial\Delta F}{\partial R}. \tag{2}$$

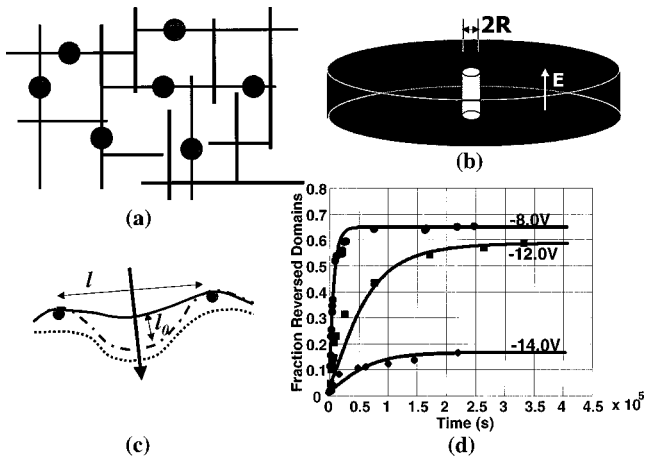

FIG. 7. (a) Schematic of the relaxation system showing random spacing of 90° domains and nucleation sites halfway on the lines. (b) Geometry of reversing nucleus. (c) Schematic of the 180° domain wall showing pinning sites and the parameters l and l_0. (d) Fit of Eq. (5) to the data for various write voltages with K and α as fitting parameters.

In Eq. (2), K is the kinetic coefficient, h_f is the film thickness, and ΔF is the decrease in the free energy of the system due to the formation of a stable domain given by

$$\Delta F=[2\pi R\Gamma-\pi R^2P_sE(1-f-\alpha)]h, \tag{3}$$

where Γ is the domain wall energy mentioned before. The second term expresses the interaction of the reversed domains with the mean field in the film, $E(f)$. Then

$$f_T=\frac{\Gamma}{R}-P_sE(f). \tag{4}$$

The first term in Eq. (4) is important on the last stages of relaxation when the second term has become very small. It determines the equilibrium state of a curved section of a wall pinned by point obstacles, as was discussed earlier (R is determined by the distance between pinning points).

At small $E(f)$ the first term can be neglected because the reversed domains nucleate on twins. Then Eqs. (1)–(4) lead to the following kinetic equation:

$$f(t)=1-\exp\left[-\left(\beta\int_0^{\xi}[1-\alpha-f(\xi)]d\xi\right)^2\right], \tag{5}$$

where $\beta=\pi KP_sE\sqrt{N}$. This equation describes the experimentally observed kinetics with α and β as the fitting parameters. The kinetic coefficients can be estimated[16,17] as below:

$$K=l_0\frac{\nu v_a}{kT}e^{-U/kT}, \tag{6}$$

where ν is the frequency of the wall vibration given by $\nu\approx\nu_{at}\,a/l$ where ν_{at} is the atomic frequency ($\nu_{at}=10^{12}\,s^{-1}$, a is the interatomic distance, l is the distance between the pinning points, v_a is the activation volume ($v_a\sim l^3$), and U is the activation energy. $l_0\approx l$ is the elementary displacement of the wall during the activation event. We can measure N, the

TABLE I. Variation of N, α, K, and U_a as a function of write voltage.

Write voltage (V)	Nucleation density, N (m^{-2})	α	K ($m^4/J\,s$)	U_a (eV)
−8.0	8.89×10^{12}	0.35	1.43×10^{-17}	0.9076
−10.0	7.77×10^{12}	0.40	2.38×10^{-18}	0.9522
−12.0	1.89×10^{12}	0.82	8.89×10^{-18}	0.9249
−14.0	5.51×10^{11}	0.87	2.38×10^{-17}	0.8949

nucleation density, from the experimental data, and taking $P_s=0.6\,C/m^2$, and $E_i=3.5\times10^6$ V/m, we can find for the −8.0-V write experiment, $K=1.48\times10^{-17}\,m^4\,J^{-1}\,s^{-1}$ [from the fit to the data of Eq. (5) as seen in Fig. 7(d)] and for $l\approx10$ nm (as seen in Ref. 18 from transmission electron microscopy of similar films) and $T\approx300$ K, we obtain $U\approx1$ eV. Table I lists the variation of N, α, K, and U_a as a function of the write voltage, while α and N are plotted in Fig. 8 as a function of write voltage.

It is to be noted that since localized effects of wall curvature and faceting on the movement of growing 180° domains are not included in the model, the fit of Eq. (6) to the data [Fig. 7(d)] will not reflect these phenomena and as a consequence is not very good at very short and very long times for various write voltages. The set of equations above also does not take into account the change in mobility of the domain walls and therefore cannot describe the saturation stage accurately. Consequently the thermodynamic parameter α can be determined only approximately. The question of the nature of relaxation saturation (thermodynamics versus kinetics) is fundamental for understanding this phenomena. Therefore additional investigation on the evolution of the built-in field is necessary to support the theoretical approach presented in this paper.

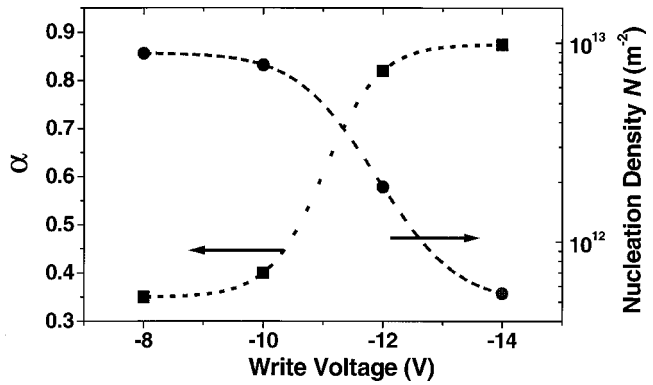

FIG. 8. Plot of α and N as a function of write voltage.

In summary, we have investigated domain structure and polarization relaxation in PZT thin films on LSCO electrodes. The JMAK model for phase change kinetics has been applied to describe the observed transformation-time data for 180° domain reversal under constantly decaying imprint driving field. The effect of local curvature on driving the domain relaxation kinetics has been studied, and it has been observed that the curvature of growing domains decreases until faceting can be clearly observed. The domain wall is seen to facet along the low-index (110) and (100) types of planes. Pinning and bowing of 180° domain walls are observed in the late stages of relaxation.

ACKNOWLEDGEMENTS

This work was supported by the NSF under Grant Nos. DMR 9632521 and No. DMR 9903279.

*Email address: chandan@glue.umd.edu
†Email address: roytburd@wam.umd.edu
‡Email address: rrl36@umail.umd.edu

[1] J. F. Scott, *Ferroelectric Memories*, Vol. 3 of the Springer Series on Advanced Microelectronics (Springer, Heidelberg, 2000).
[2] T. Hidaka, T. Mayurama, M. Saitoh, N. Mikoshiba, M. Shimizu, T. Shiosaki, L. A. Wills, R. Hiskes, S. A. Dicarolis, and J. Amano, Appl. Phys. Lett. **68**, 2358 (1996); C. H. Ahn, T. Tybell, L. Antognazza, K. Char, R. H. Hammond, M. R. Beasley, Ø. Fisher, and J.-M. Triscone, Science **276**, 1100 (1997).
[3] A. Gruverman, H. Tokumoto, A. S. Prakash, S. Aggarwal, B. Yang, M. Wuttig, R. Ramesh, O. Auciello, and T. Venkatesan, Appl. Phys. Lett. **71**, 3492 (1997).
[4] C. S. Ganpule, V. Nagarajan, S. B. Ogale, A. L. Roytburd, E. D. Williams, and R. Ramesh, Appl. Phys. Lett. **77**, 3275 (2000).
[5] C. S. Ganpule, V. Nagarajan, H. Li, A. S. Ogale, D. E. Steinhauer, S. Aggarwal, E. Williams, and R. Ramesh, Appl. Phys. Lett. **77**, 292 (2000).
[6] J. D. Axe and Y. Yamada, Phys. Rev. B **34**, 1599 (1986); K. Sekimoto, Physica A **125**, 261 (1984); **128**, 132 (1984); **135**, 328 (1986); S. Ohta, T. Ohta, and K. Kawasaki, *ibid.* **140**, 478 (1987); R. M. Bradly and P. N. Strenski, Phys. Rev. B **40**, 8967 (1989); K. Sekimoto, Int. J. Mod. Phys. B **5**, 1843 (1991); Y. A. Andrienko, N. V. Brilliantov, and P. V. Krapivsky, Phys. Rev. A **45**, 2263 (1992).
[7] G. E. Pike, W. L. Warren, D. Dimos, B. A. Tuttle, R. Ramesh, J. Lee, V. G. Keramidas, and J. T. Evans, Jr., Appl. Phys. Lett. **66**, 484 (1995).
[8] P. Güthner and K. Dransfeld, Appl. Phys. Lett. **61**, 1137 (1992); A. Gruverman, O. Auciello, and H. Tokumoto, *ibid.* **69**, 3191 (1996); T. Tybell, C. H. Ahn, and J.-M. Triscone, *ibid.* **72**, 1454 (1998); O. Auciello, A. Gruverman, H. Tokumoto, S. A. Prakash, S. Aggarwal, and R. Ramesh, Mater. Res. Bull. **23**, 33 (1998).
[9] A. L. Roytburd, Phys. Status Solidi A **37**, 329 (1976).
[10] V. Nagarajan, I. G. Jenkins, S. P. Alpay, H. Li, S. Aggarwal, L. Salamanca-Riba, A. L. Roytburd, and R. Ramesh, J. Appl. Phys. **86**, 595 (1999).
[11] A. J. Bray, Adv. Phys. **43**, 357 (1994).
[12] T. J. Yang, Venkatraman Gopalan, P. J. Swart, and U. Mohideen, Phys. Rev. Lett. **82**, 4106 (1999).
[13] J. M. Benedetto, R. A. Moore, and F. B. McLean, J. Appl. Phys. **75**, 460 (1994); W. Jo, D. C. Kim and J. W. Hong, Appl. Phys. Lett. **76**, 390 (2000).
[14] J. Kakilios, R. A. Street, and W. B. Jackson, Phys. Rev. Lett. **59**, 1037 (1987); R. G. Palmer, D. L. Stein, E. Abrahams, and P. W. Anderson, *ibid.* **53**, 958 (1984); R. V. Chamberlin, G. Mo-

zurkewich, and R. Orbach, *ibid.* **52**, 867 (1984); D. K. Lottis, R. M. White, and E. Dan Dahlberg, *ibid.* **67**, 362 (1991).
[15] A. Gruverman and M. Tanaka, J. Appl. Phys. **89**, 1836 (2001).
[16] Paul G. Shewmon, *Transformations in Metals* (McGraw-Hill, New York, 1969); B. Y. Lyubov, *Kinetic Theory of Phase Transformation* (National Bureau of Standards, New Delhi, 1978).
[17] A. L. Roytburd, E. V. Safonov, T. M. Siritskaya, and A. V. Shalinova, Kristallografiya **22**, 307 (1977).
[18] H. Li, L. Salamanca-Riba, and R. Ramesh (unpublished).